Different periodic behaviours of magnetic helicity flux in flaring and non-flaring AR cases

Sz. Soós,[1,4] M. B. Korsós,[2,1,4] H. Morgan,[2] and R. Erdélyi[3,1,4]

[1] Department of Astronomy, Eötvös Loránd University

[2] Department of Physics, Aberystwyth University

[3] Solar Physics & Space Plasma Research Center (SP2RC), U. of Sheffield

[4] Hungarian Solar Physics Foundation (HSPF)

Importance of Space Weather

- Solar flares and Coronal Mass Ejections (CMEs) have **dominant roles** in space weather (Eastwood et al. 2017, Temmer 2021).

Importance of Space Weather

- Solar flares and Coronal Mass Ejections (CMEs) have **dominant roles** in space weather (Eastwood et al. 2017, Temmer 2021).
- It is vital to further **develop existing prediction capabilities** through the identification of observable precursors of flares and CMEs.

Importance of Space Weather

- Solar flares and Coronal Mass Ejections (CMEs) have **dominant roles** in space weather (Eastwood et al. 2017, Temmer 2021).
- It is vital to further **develop existing prediction capabilities** through the identification of observable precursors of flares and CMEs.
- Understanding the physical processes of **precursors** is still a challenging task.

Importance of Space Weather

- Solar flares and Coronal Mass Ejections (CMEs) have **dominant roles** in space weather (Eastwood et al. 2017, Temmer 2021).
- It is vital to further **develop existing prediction capabilities** through the identification of observable precursors of flares and CMEs.
- Understanding the physical processes of **precursors** is still a challenging task.
- The most intense solar eruptions originate from the most magnetically complex, and highly twisted **δ-type active regions** (Georgoulis et al. 2019).

Importance of Space Weather

- Solar flares and Coronal Mass Ejections (CMEs) have **dominant roles** in space weather (Eastwood et al. 2017, Temmer 2021).
- It is vital to further **develop existing prediction capabilities** through the identification of observable precursors of flares and CMEs.
- Understanding the physical processes of **precursors** is still a challenging task.
- The most intense solar eruptions originate from the most magnetically complex, and highly twisted **δ-type active regions** (Georgoulis et al. 2019).
- Focus on the observational property of **magnetic helicity flux** in δ-type ARs.

Magnetic helicity flux

- Elsasser (1956) and Woltjer (1958) the **magnetic helicity**:

$$H = \int_V \vec{A} \cdot \vec{B} d^3x$$

- H is conserved in iMHD, when the volume of integration is bounded by a magnetic surface.

Magnetic helicity flux

- Elsasser (1956) and Woltjer (1958) the **magnetic helicity**:

$$H = \int_V \vec{A} \cdot \vec{B} d^3x$$

- H is conserved in iMHD, when the volume of integration is bounded by a magnetic surface.
- H arises from the topological properties of the field, i.e., from the linking, knotting, and twisting of field lines.

Magnetic helicity flux

- Elsasser (1956) and Woltjer (1958) the **magnetic helicity**:

$$H = \int_V \vec{A} \cdot \vec{B} d^3x$$

- H is conserved in iMHD, when the volume of integration is bounded by a magnetic surface.
- H arises from the topological properties of the field, i.e., from the linking, knotting, and twisting of field lines.
- Berger (1984):

$$\left.\frac{dH}{dt}\right|_S = 2\int_S (\vec{A}_p \cdot \vec{B}_h)\vec{v}_{\perp z} dS - 2\int_S (\vec{A}_p \cdot \vec{v}_{\perp h})\vec{B}_z dS$$

Magnetic helicity flux

- *Korsós et al. (2020)*:

$$T \equiv \left.\frac{dH}{dt}\right|_S = 2\int_S \underbrace{(\vec{A}_p \cdot \vec{B}_h)\vec{v}_{\perp z} dS}_{EM} - 2\int_S \underbrace{(\vec{A}_p \cdot \vec{v}_{\perp h})\vec{B}_z dS}_{SH}$$

Magnetic helicity flux

- *Korsós et al. (2020)*:

$$T \equiv \left.\frac{dH}{dt}\right|_S = 2\int_S \underbrace{(\vec{A}_p \cdot \vec{B}_h)\vec{v}_{\perp z} dS}_{EM} - 2\int_S \underbrace{(\vec{A}_p \cdot \vec{v}_{\perp h})\vec{B}_z dS}_{SH}$$

- *EM* comes from the twisted magnetic flux tubes emerging into the solar atmosphere.

Magnetic helicity flux

- *Korsós et al. (2020)*:

$$T \equiv \left.\frac{dH}{dt}\right|_S = 2\int_S \underbrace{(\vec{A}_p \cdot \vec{B}_h)\vec{v}_{\perp z} dS}_{EM} - 2\int_S \underbrace{(\vec{A}_p \cdot \vec{v}_{\perp h})\vec{B}_z dS}_{SH}$$

- *EM* comes from the twisted magnetic flux tubes emerging into the solar atmosphere.
- *SH* comes from the shearing and braiding of the field lines, which is caused by the tangential motions on the solar surface.

Magnetic helicity flux

- *Korsós et al. (2020)*:

$$T \equiv \left.\frac{dH}{dt}\right|_S = 2\int_S \underbrace{(\vec{A}_p \cdot \vec{B}_h)\vec{v}_{\perp z} dS}_{EM} - 2\int_S \underbrace{(\vec{A}_p \cdot \vec{v}_{\perp h})\vec{B}_z dS}_{SH}$$

- *EM* comes from the twisted magnetic flux tubes emerging into the solar atmosphere.
- *SH* comes from the shearing and braiding of the field lines, which is caused by the tangential motions on the solar surface.
- Investigated the evolution of EM/SH/T for **3 flaring and 3 non-flaring ARs**.

Magnetic helicity flux

- *Korsós et al. (2020)*:

$$T \equiv \left.\frac{dH}{dt}\right|_S = 2\int_S \underbrace{(\vec{A}_p \cdot \vec{B}_h)\vec{v}_{\perp z} dS}_{EM} - 2\int_S \underbrace{(\vec{A}_p \cdot \vec{v}_{\perp h})\vec{B}_z dS}_{SH}$$

- *EM* comes from the twisted magnetic flux tubes emerging into the solar atmosphere.
- *SH* comes from the shearing and braiding of the field lines, which is caused by the tangential motions on the solar surface.
- Investigated the evolution of EM/SH/T for **3 flaring and 3 non-flaring ARs**.
- Relationship between the oscillatory behavior of EM/SH/T and the associated flare activities.

Magnetic helicity flux

- *Korsós et al. (2020)*:

$$T \equiv \left.\frac{dH}{dt}\right|_S = 2\int_S \underbrace{(\vec{A}_p \cdot \vec{B}_h)\vec{v}_{\perp z} dS}_{EM} - 2\int_S \underbrace{(\vec{A}_p \cdot \vec{v}_{\perp h})\vec{B}_z dS}_{SH}$$

- *EM* comes from the twisted magnetic flux tubes emerging into the solar atmosphere.
- *SH* comes from the shearing and braiding of the field lines, which is caused by the tangential motions on the solar surface.
- Investigated the evolution of EM/SH/T for **3 flaring and 3 non-flaring ARs**.
- Relationship between the oscillatory behavior of EM/SH/T and the associated flare activities.
- *Their **conjecture** was that EM/SH/T have a common period before flare onset.*

Data

- **Random sample** of 14 flaring and 14 non-flaring Ars.

  (**SHARP – hmi.sharp_cea_720s**)

- The ARs are **selected** based on the following criteria:

Data

- **Random sample** of 14 flaring and 14 non-flaring Ars.

  (**SHARP – hmi.sharp_cea_720s**)

- The ARs are **selected** based on the following criteria:
  - the **angular distance** of an AR from the central meridian is **±60°**, to obtain the best possible quality data (Bobra et al. 2014).

Data

- **Random sample** of 14 flaring and 14 non-flaring Ars.

  (**SHARP – hmi.sharp_cea_720s**)

- The ARs are **selected** based on the following criteria:
  - the **angular distance** of an AR from the central meridian is **±60°**, to obtain the best possible quality data (Bobra et al. 2014).
  - the AR must have a **δ-spot** configuration.

Data

- **Random sample** of 14 flaring and 14 non-flaring Ars.

  (**SHARP – hmi.sharp_cea_720s**)

- The ARs are **selected** based on the following criteria:
  - the **angular distance** of an AR from the central meridian is **±60°**, to obtain the best possible quality data (Bobra et al. 2014).
  - the AR must have a **δ-spot** configuration.
  - the flaring ARs must be the location of **at least one X-class flare**.

Data

- **Random sample** of 14 flaring and 14 non-flaring Ars.

  (**SHARP – hmi.sharp_cea_720s**)

- The ARs are **selected** based on the following criteria:
  - the **angular distance** of an AR from the central meridian is **±60°**, to obtain the best possible quality data (Bobra et al. 2014).
  - the AR must have a **δ-spot** configuration.
  - the flaring ARs must be the location of **at least one X-class flare**.
  - the non-flaring ARs should not be the host of flares larger than M5.

Data

- **Random sample** of 14 flaring and 14 non-flaring Ars.

  (**SHARP – hmi.sharp_cea_720s**)

- The ARs are **selected** based on the following criteria:
  - the **angular distance** of an AR from the central meridian is **±60°**, to obtain the best possible quality data (Bobra et al. 2014).
  - the AR must have a **δ-spot** configuration.
  - the flaring ARs must be the location of **at least one X-class flare**.
  - the non-flaring ARs should not be the host of flares larger than M5.
  - the AR cannot be associated with fast CMEs (Here, we define ≥750 km s^{-1}).

Wavelet analysis

- Wavelet analysis on **both original and smoothed time series** of EM/SH/T.

Wavelet analysis

- Wavelet analysis on **both original and smoothed time series** of EM/SH/T.
- **Smoothing** was done by 24 hrs that was subtracted from the original data in order to damp out the 12 and 24 hrs SDO artifact (Smirnova et al. 2013).

Wavelet analysis

- Wavelet analysis on **both original and smoothed time series** of EM/SH/T.
- **Smoothing** was done by 24 hrs that was subtracted from the original data in order to damp out the 12 and 24 hrs SDO artifact (Smirnova et al. 2013).
- From the wavelet power spectrum (WPS), global power spectra (GPS) are calculated through averaging the WPS over time.
- **1σ level**.

Wavelet analysis

- Wavelet analysis on **both original and smoothed time series** of EM/SH/T.
- **Smoothing** was done by 24 hrs that was subtracted from the original data in order to damp out the 12 and 24 hrs SDO artifact (Smirnova et al. 2013).
- From the wavelet power spectrum (WPS), global power spectra (GPS) are calculated through averaging the WPS over time.
- **1σ level**.
- **Local maxima** in the WPS using an implementation of the 0-th dimensional persistent homology method (Huber 2021).

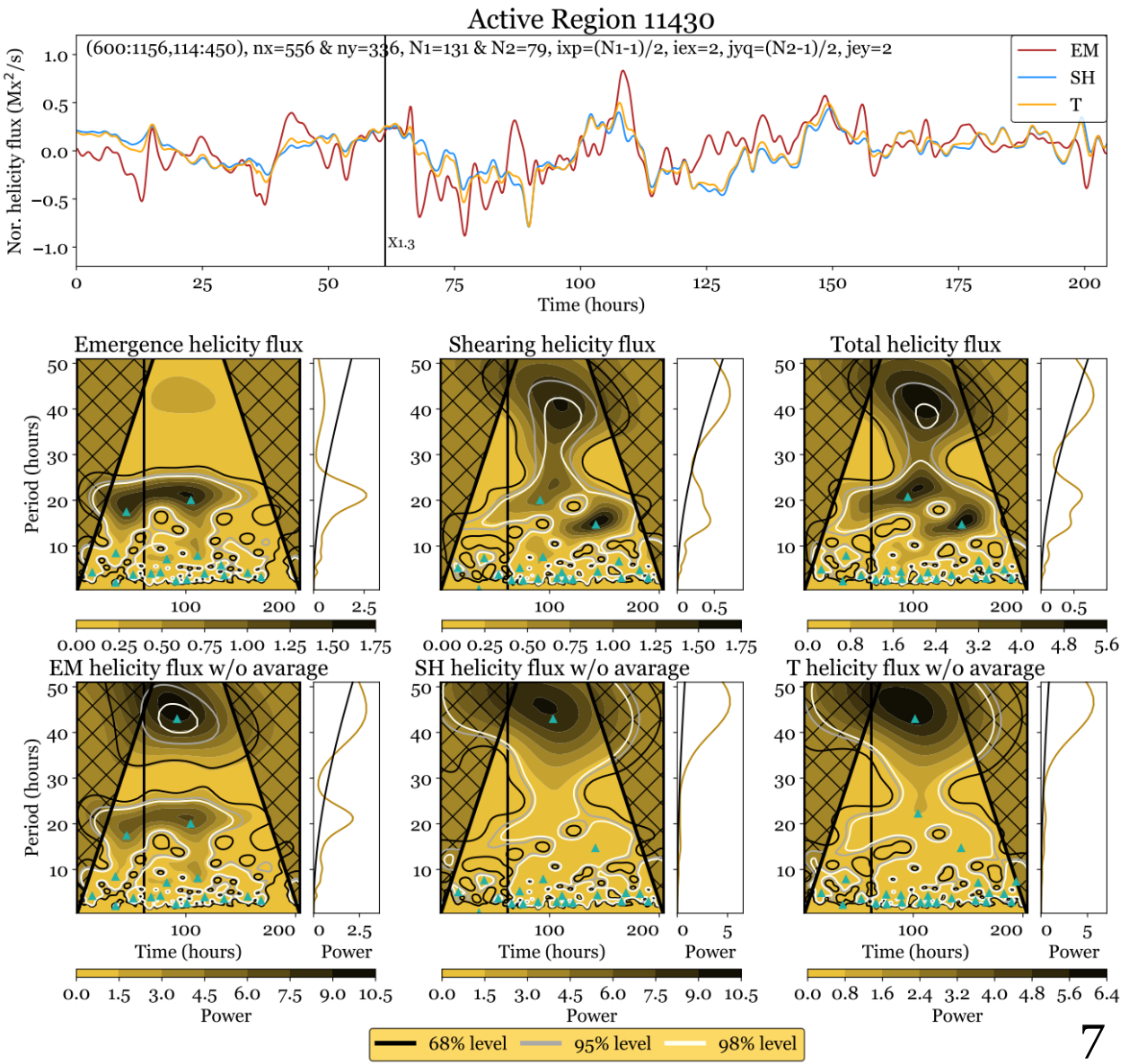
Active Region 11430
(600:1156,114:450), nx=556 & ny=336, N1=131 & N2=79, ixp=(N1-1)/2, iex=2, jyq=(N2-1)/2, jey=2
EM
SH
T
Nor. helicity flux (Mx²/s)
X1.3
Time (hours)
Emergence helicity flux
Shearing helicity flux
Total helicity flux
Period (hours)
EM helicity flux w/o avarage
SH helicity flux w/o avarage
T helicity flux w/o avarage
Time (hours)
Power
68% level
95% level
98% level

ELTE EÖTVÖS LORÁND TUDOMÁNYEGYETEM

X1.3 flare

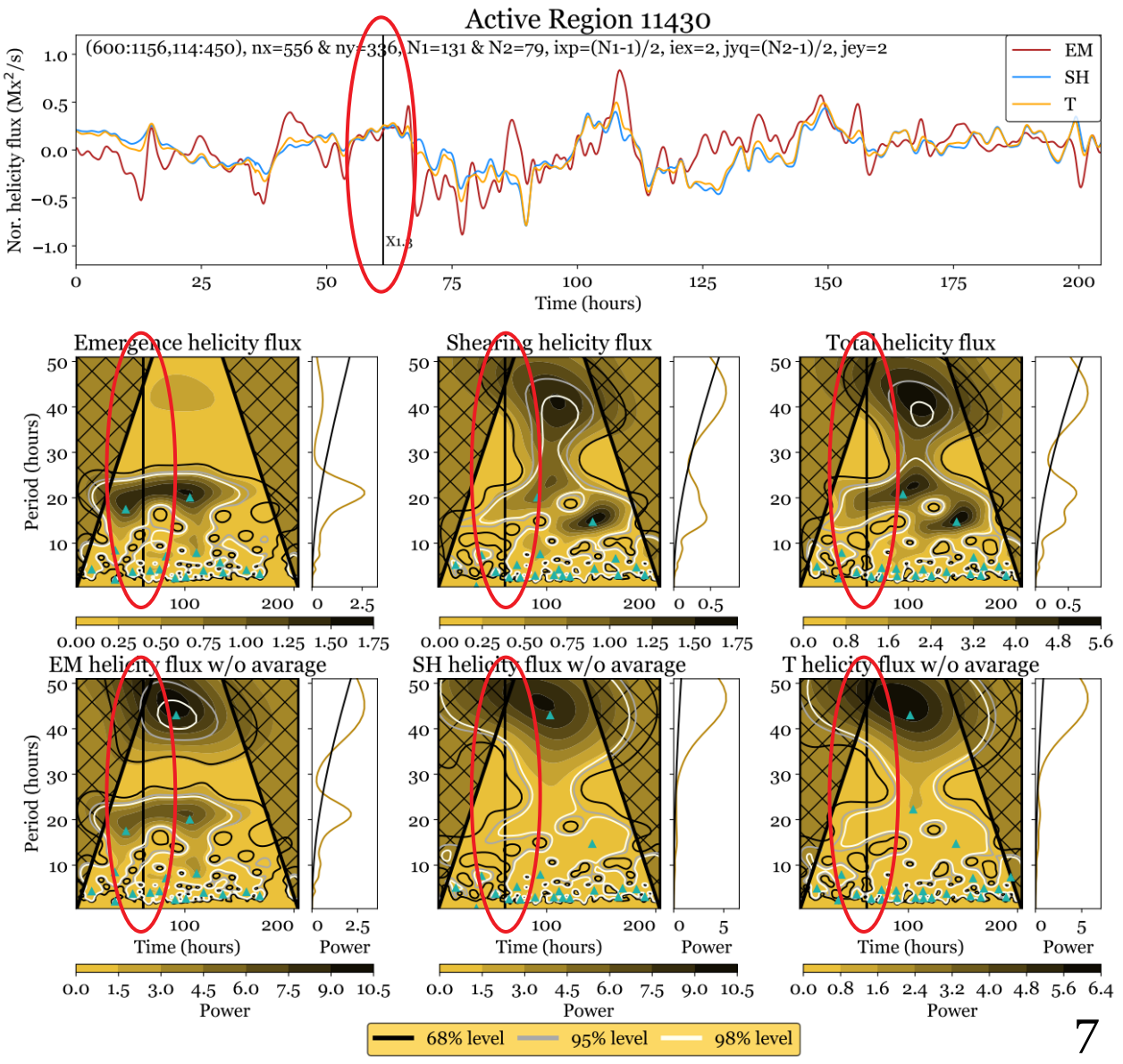

ELTE EÖTVÖS LORÁND TUDOMÁNYEGYETEM

X1.3 flare

Unsmoothed EM/SH/T time series

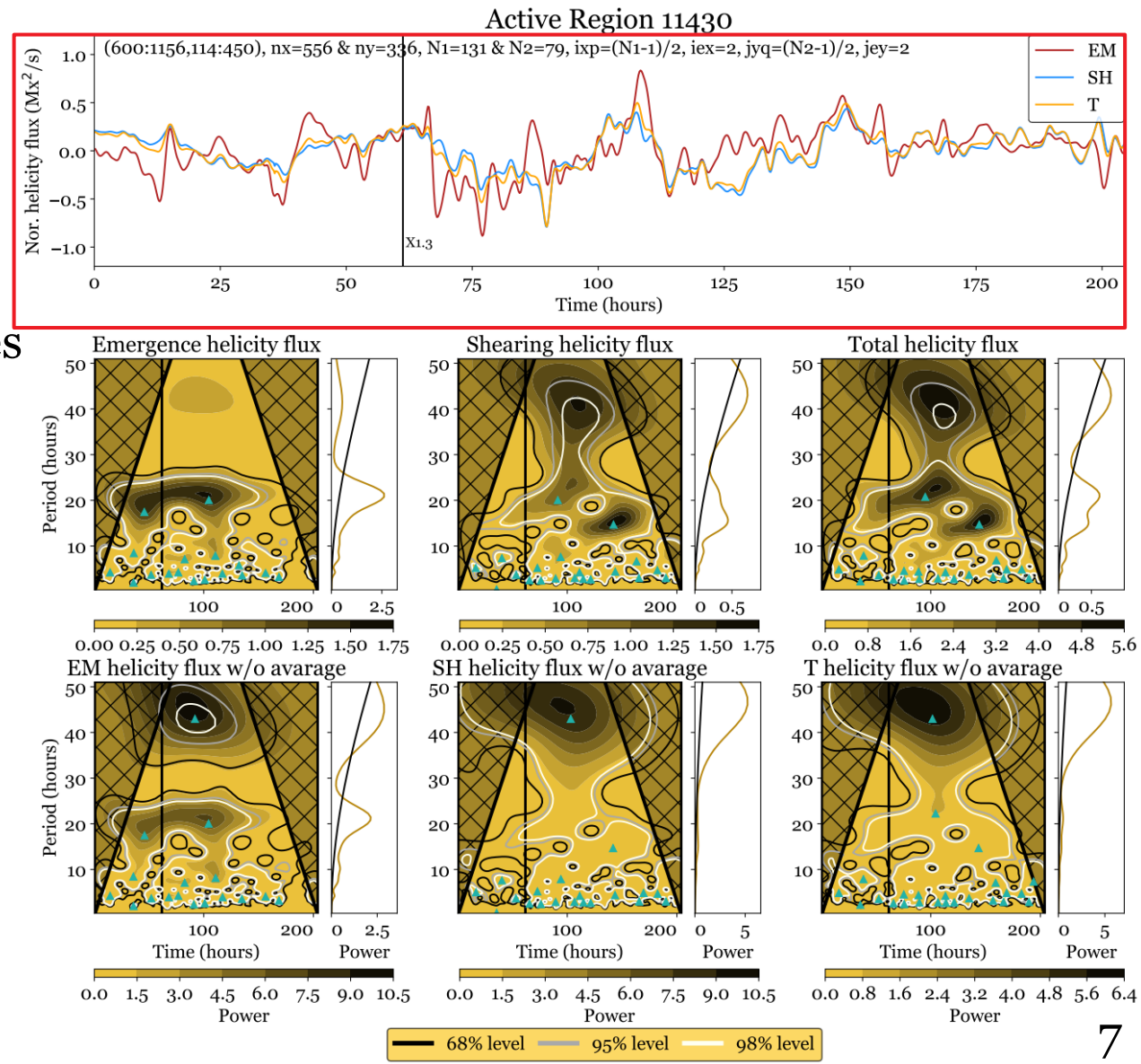

ELTE EÖTVÖS LORÁND TUDOMÁNYEGYETEM

X1.3 flare

Unsmoothed EM/SH/T time series

WPS of the smoothed EM/SH/T

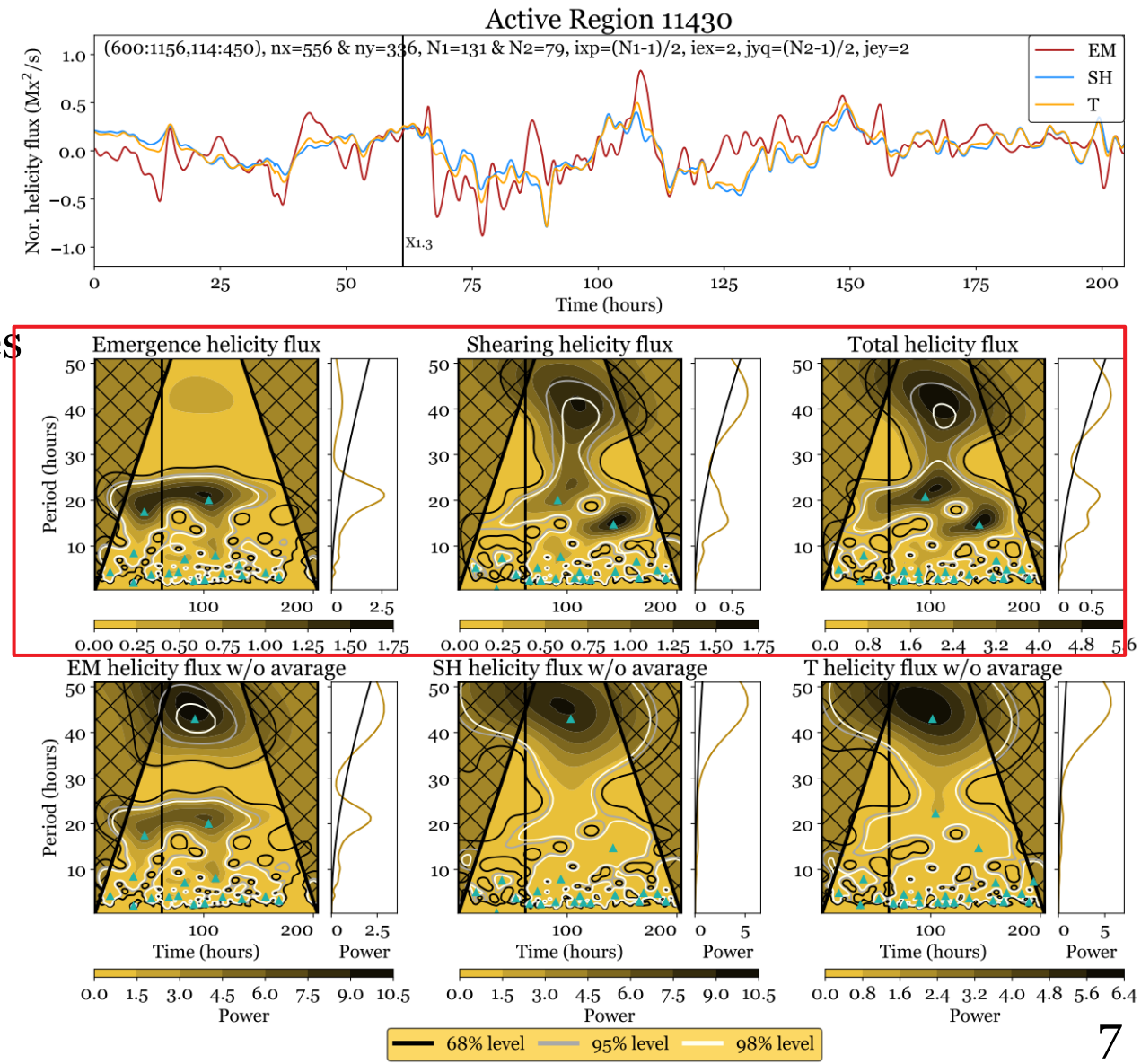

ELTE EÖTVÖS LORÁND TUDOMÁNYEGYETEM

X1.3 flare

Unsmoothed EM/SH/T time series

WPS of the smoothed EM/SH/T

WPS of the unsmoothed EM/SH/T

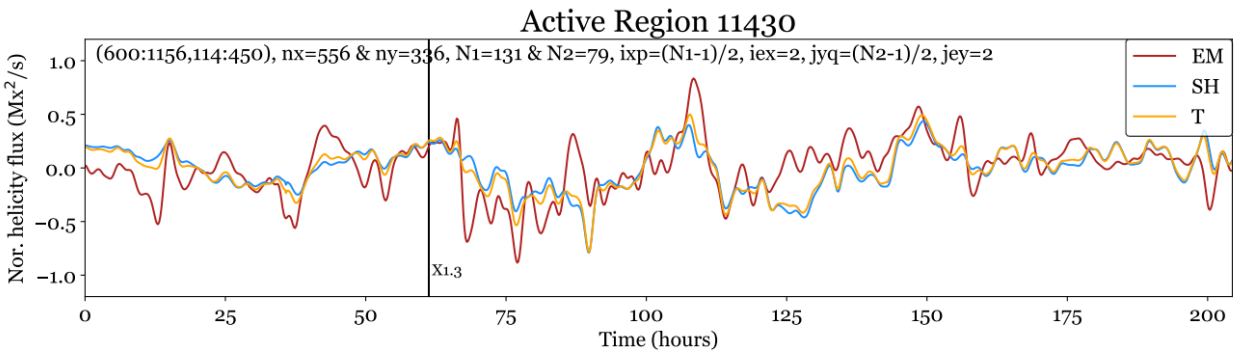

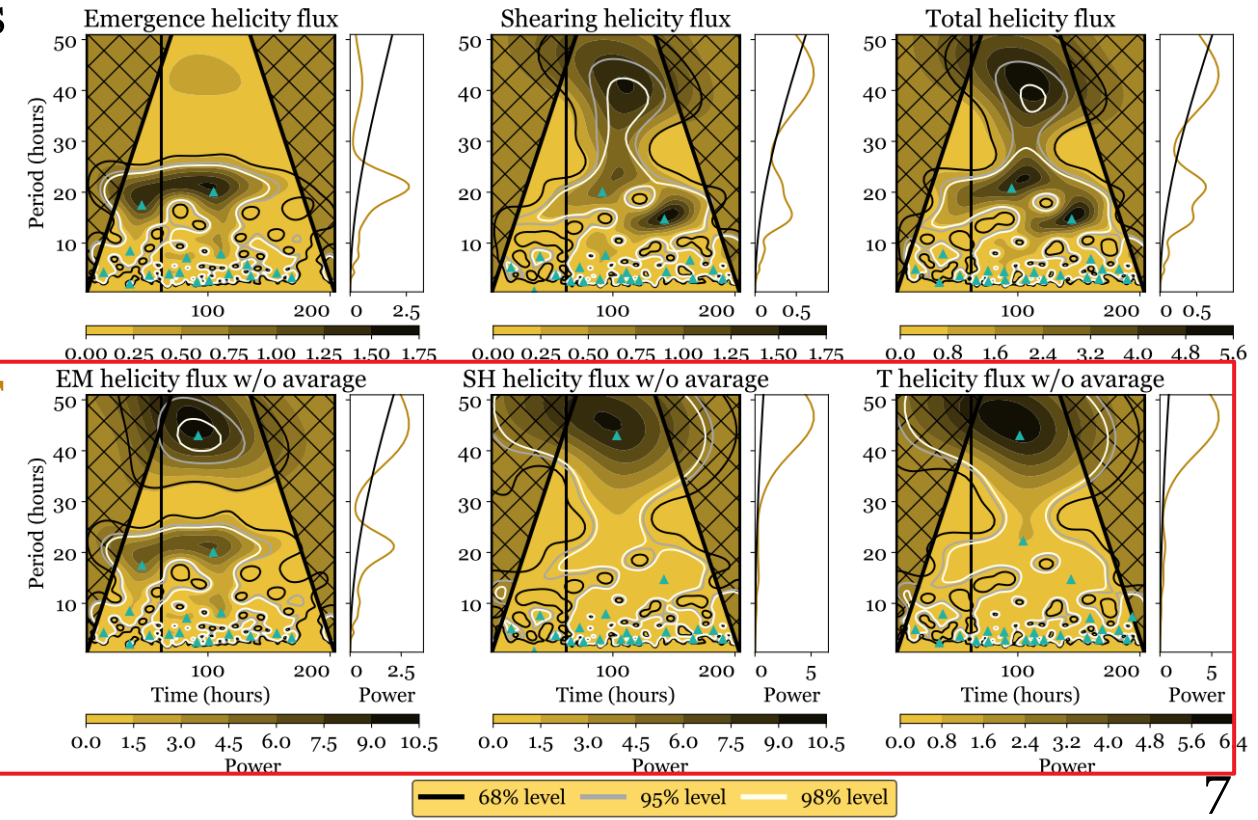

ELTE EÖTVÖS LORÁND TUDOMÁNYEGYETEM

X1.3 flare

Unsmoothed EM/SH/T time series

WPS of the smoothed EM/SH/T

WPS of the unsmoothed EM/SH/T

Right of each WPS are the GPS

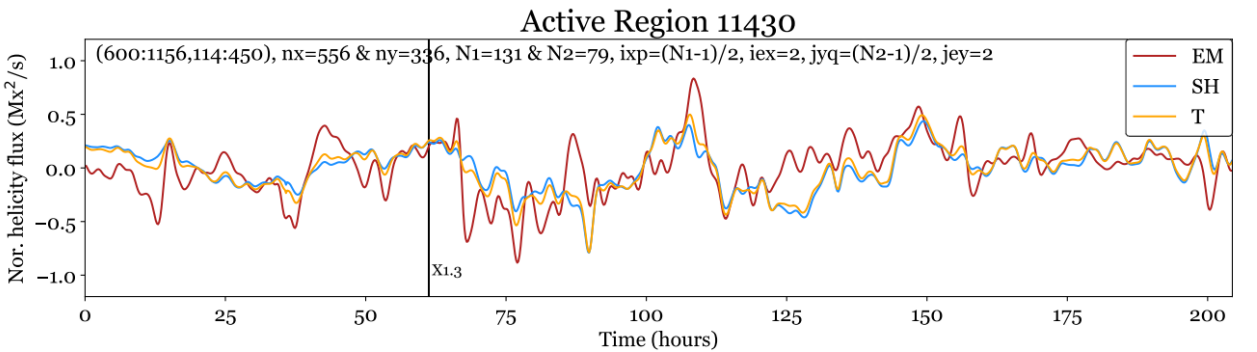

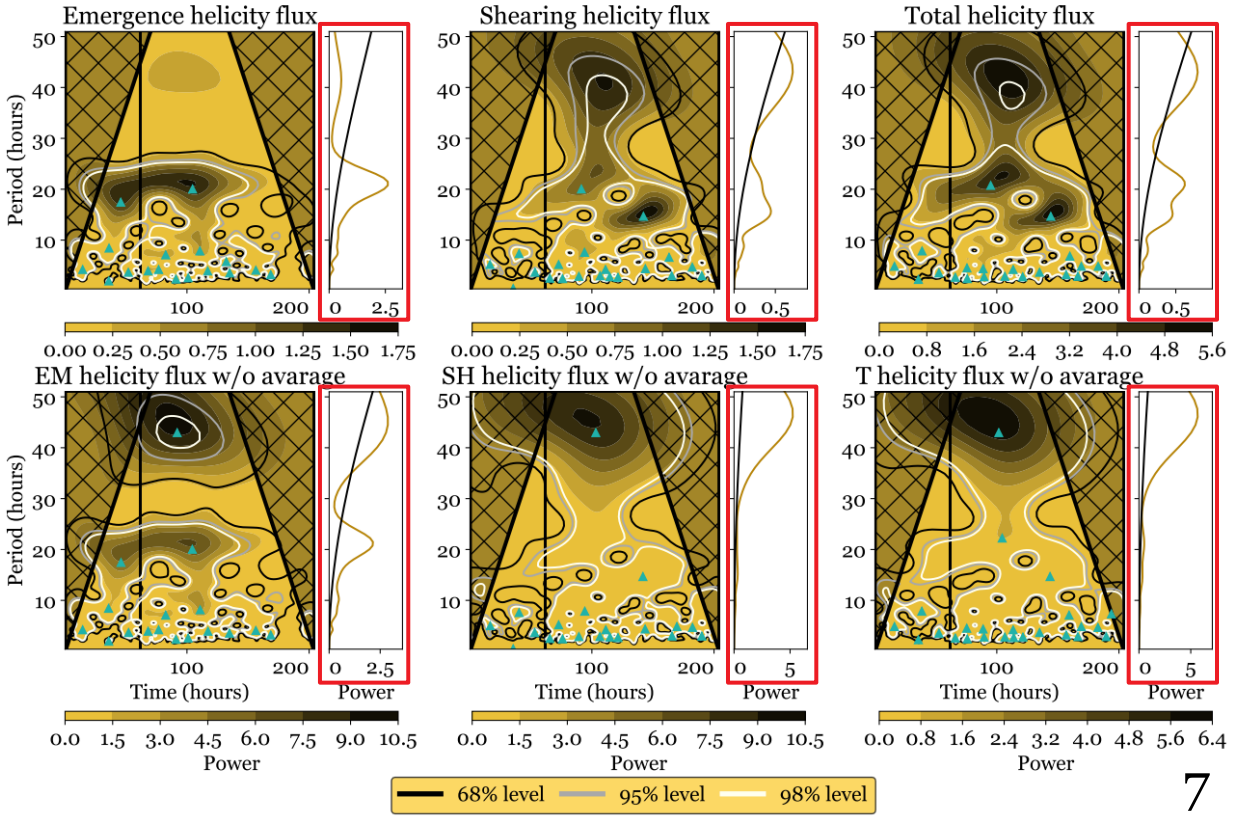

ELTE EÖTVÖS LORÁND TUDOMÁNYEGYETEM

X1.3 flare

Unsmoothed EM/SH/T time series

WPS of the smoothed EM/SH/T

WPS of the unsmoothed EM/SH/T

Right of each WPS are the GPS

Significance levels,

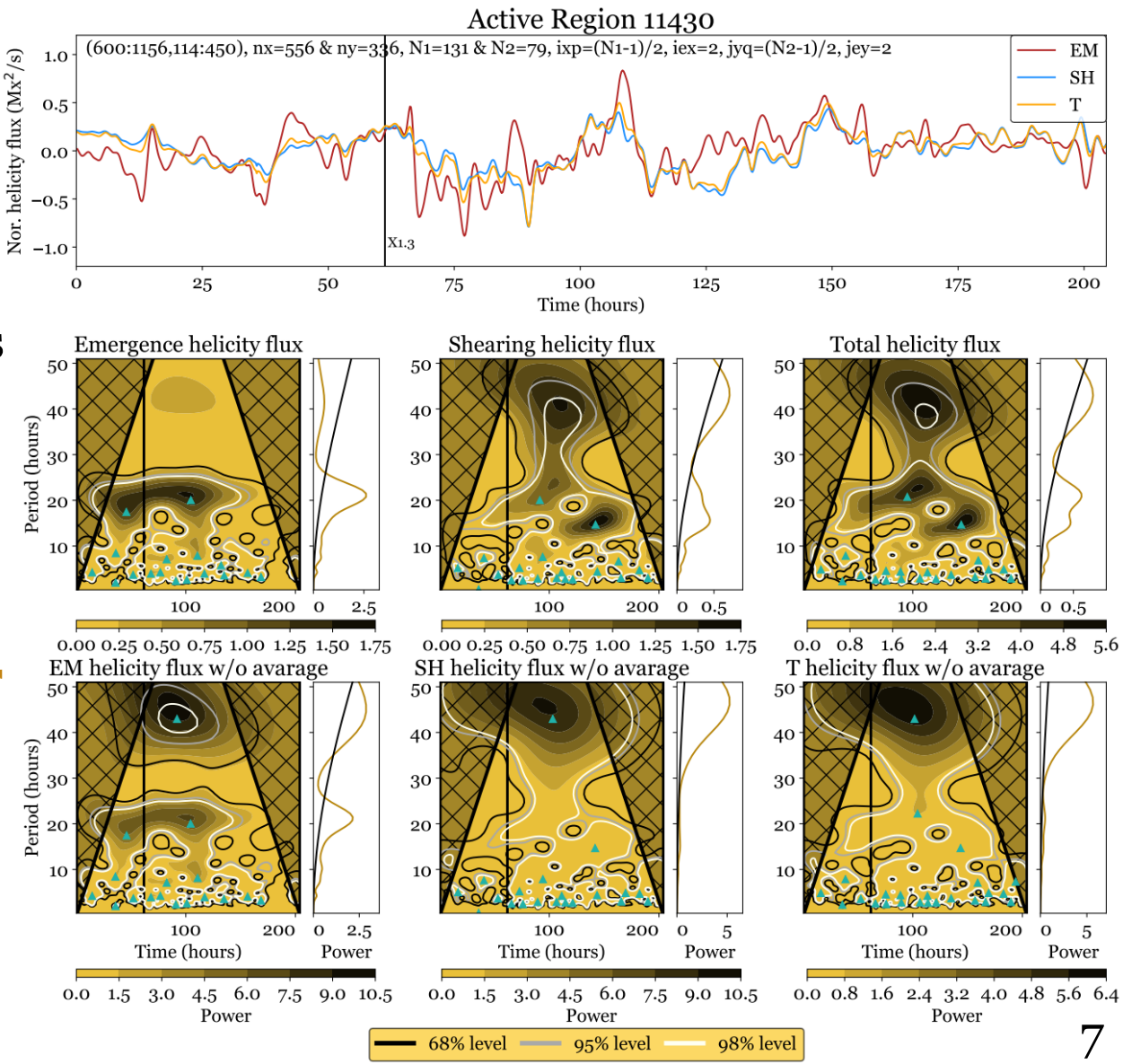

ELTE EÖTVÖS LORÁND TUDOMÁNYEGYETEM

X1.3 flare

Unsmoothed EM/SH/T time series

WPS of the smoothed EM/SH/T

WPS of the unsmoothed EM/SH/T

Right of each WPS are the GPS

Significance levels, power,

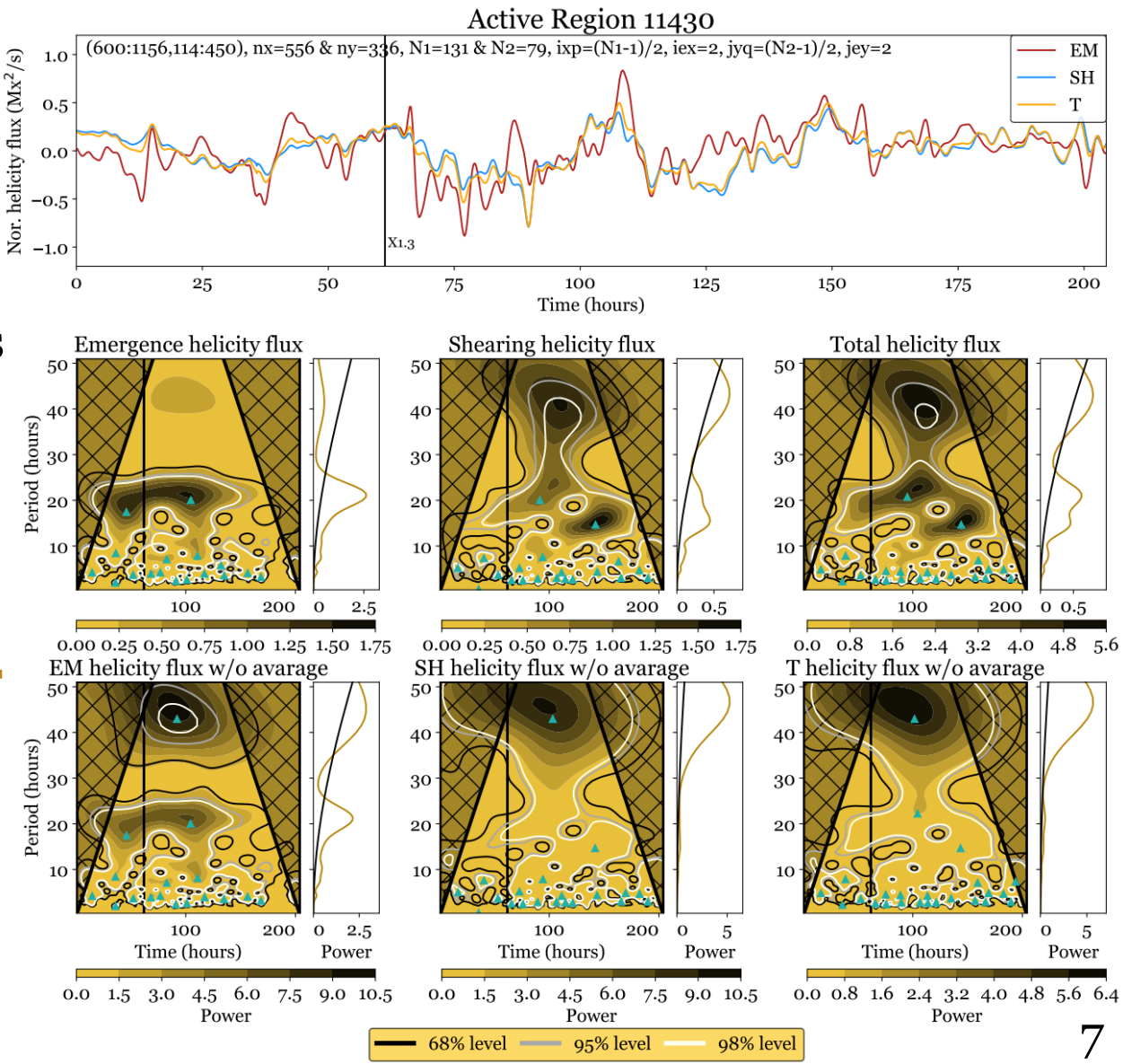

ELTE EÖTVÖS LORÁND TUDOMÁNYEGYETEM

X1.3 flare

Unsmoothed EM/SH/T time series

WPS of the smoothed EM/SH/T

WPS of the unsmoothed EM/SH/T

Right of each WPS are the GPS

Significance levels, power, peaks.

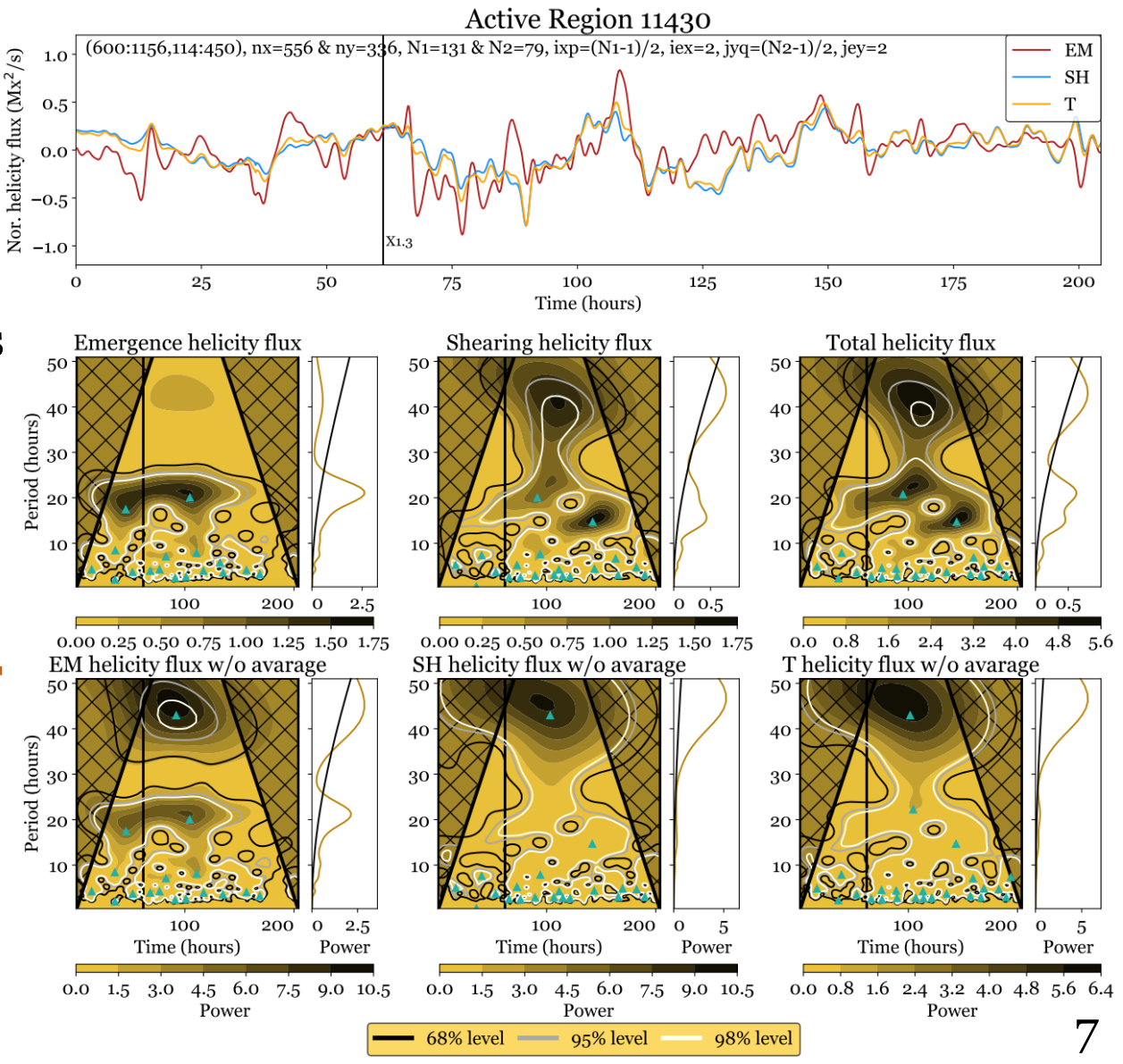

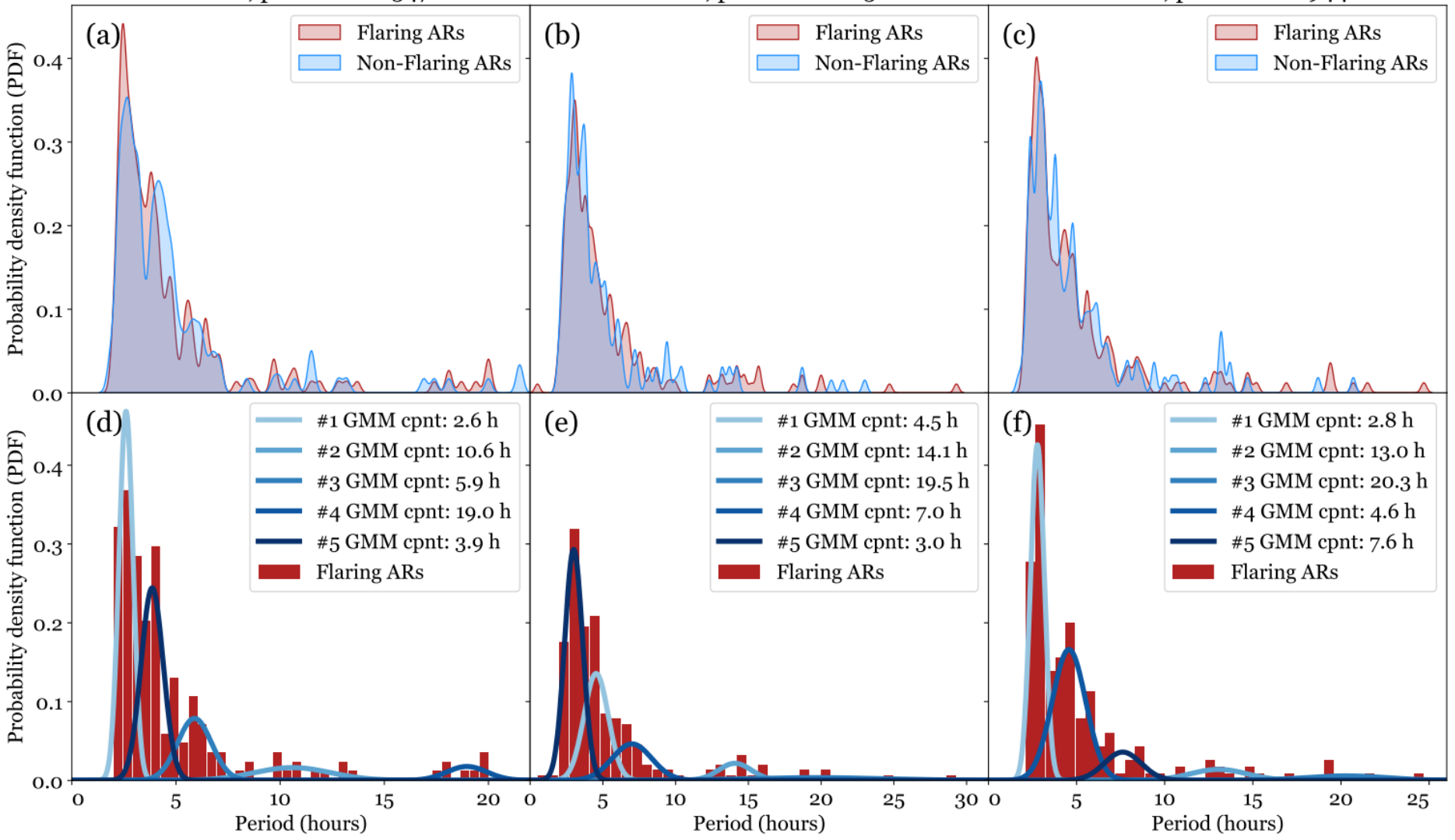
Emergence magnetic helicity flux
KS test, p-value = 0.547
Shearing magnetic helicity flux
KS test, p-value = 0.852
Total magnetic helicity flux
KS test, p-value = 0.944
(a)
(b)
(c)
Flaring ARs
Non-Flaring ARs
Probability density function (PDF)
(d)
(e)
(f)
#1 GMM cpnt: 2.6 h
#2 GMM cpnt: 10.6 h
#3 GMM cpnt: 5.9 h
#4 GMM cpnt: 19.0 h
#5 GMM cpnt: 3.9 h
#1 GMM cpnt: 4.5 h
#2 GMM cpnt: 14.1 h
#3 GMM cpnt: 19.5 h
#4 GMM cpnt: 7.0 h
#5 GMM cpnt: 3.0 h
#1 GMM cpnt: 2.8 h
#2 GMM cpnt: 13.0 h
#3 GMM cpnt: 20.3 h
#4 GMM cpnt: 4.6 h
#5 GMM cpnt: 7.6 h
Period (hours)

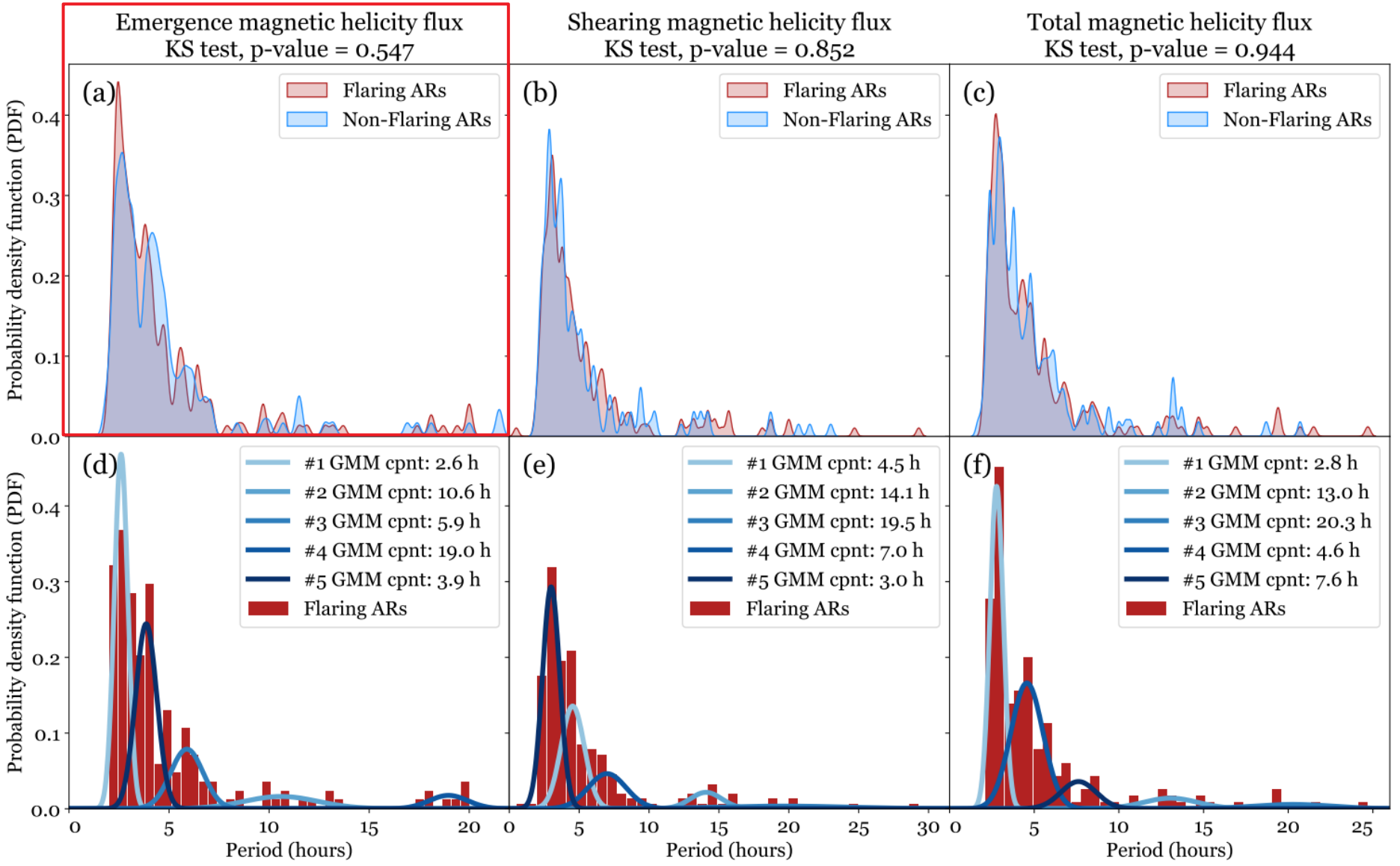
Emergence magnetic helicity flux
KS test, p-value = 0.547
Shearing magnetic helicity flux
KS test, p-value = 0.852
Total magnetic helicity flux
KS test, p-value = 0.944
(a)
(b)
(c)
Flaring ARs
Non-Flaring ARs
Probability density function (PDF)
(d)
(e)
(f)
#1 GMM cpnt: 2.6 h
#2 GMM cpnt: 10.6 h
#3 GMM cpnt: 5.9 h
#4 GMM cpnt: 19.0 h
#5 GMM cpnt: 3.9 h
#1 GMM cpnt: 4.5 h
#2 GMM cpnt: 14.1 h
#3 GMM cpnt: 19.5 h
#4 GMM cpnt: 7.0 h
#5 GMM cpnt: 3.0 h
#1 GMM cpnt: 2.8 h
#2 GMM cpnt: 13.0 h
#3 GMM cpnt: 20.3 h
#4 GMM cpnt: 4.6 h
#5 GMM cpnt: 7.6 h
Period (hours)

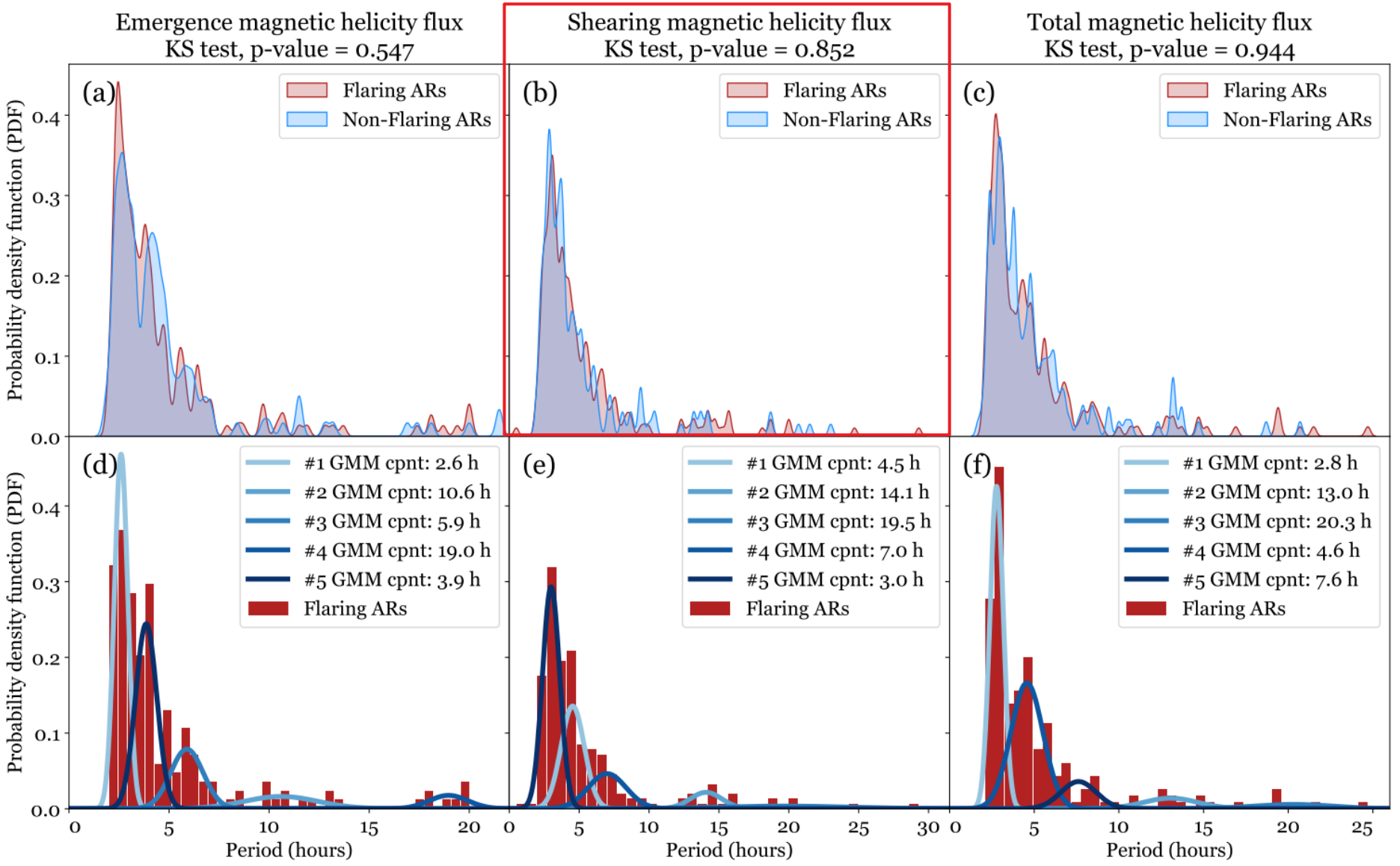
Emergence magnetic helicity flux
KS test, p-value = 0.547
Shearing magnetic helicity flux
KS test, p-value = 0.852
Total magnetic helicity flux
KS test, p-value = 0.944
(a)
(b)
(c)
Flaring ARs
Non-Flaring ARs
Probability density function (PDF)
(d)
(e)
(f)
#1 GMM cpnt: 2.6 h
#2 GMM cpnt: 10.6 h
#3 GMM cpnt: 5.9 h
#4 GMM cpnt: 19.0 h
#5 GMM cpnt: 3.9 h
#1 GMM cpnt: 4.5 h
#2 GMM cpnt: 14.1 h
#3 GMM cpnt: 19.5 h
#4 GMM cpnt: 7.0 h
#5 GMM cpnt: 3.0 h
#1 GMM cpnt: 2.8 h
#2 GMM cpnt: 13.0 h
#3 GMM cpnt: 20.3 h
#4 GMM cpnt: 4.6 h
#5 GMM cpnt: 7.6 h
Period (hours)

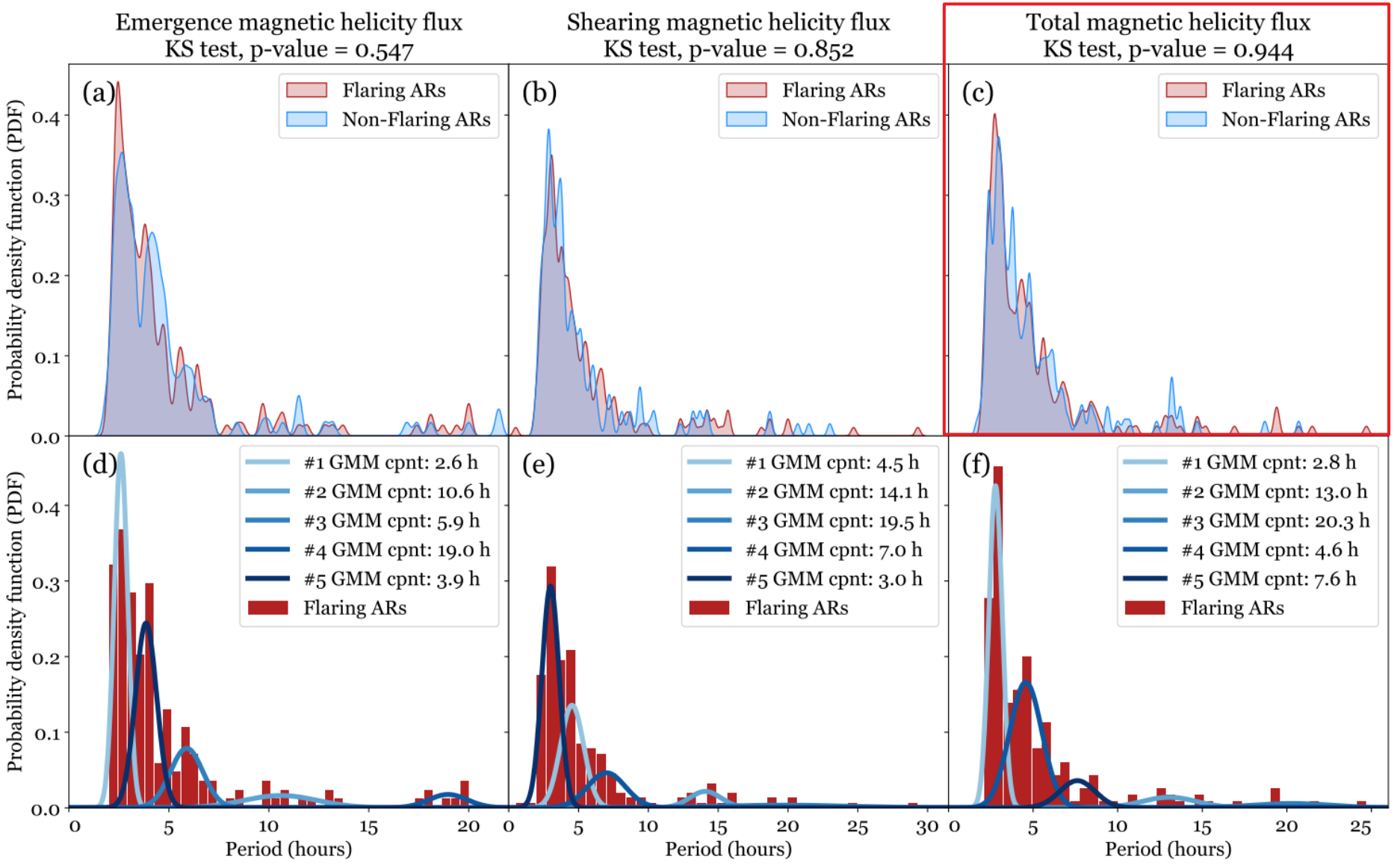
Emergence magnetic helicity flux
KS test, p-value = 0.547
Shearing magnetic helicity flux
KS test, p-value = 0.852
Total magnetic helicity flux
KS test, p-value = 0.944
(a)
(b)
(c)
Flaring ARs
Non-Flaring ARs
Probability density function (PDF)
(d)
#1 GMM cpnt: 2.6 h
#2 GMM cpnt: 10.6 h
#3 GMM cpnt: 5.9 h
#4 GMM cpnt: 19.0 h
#5 GMM cpnt: 3.9 h
(e)
#1 GMM cpnt: 4.5 h
#2 GMM cpnt: 14.1 h
#3 GMM cpnt: 19.5 h
#4 GMM cpnt: 7.0 h
#5 GMM cpnt: 3.0 h
(f)
#1 GMM cpnt: 2.8 h
#2 GMM cpnt: 13.0 h
#3 GMM cpnt: 20.3 h
#4 GMM cpnt: 4.6 h
#5 GMM cpnt: 7.6 h
Period (hours)

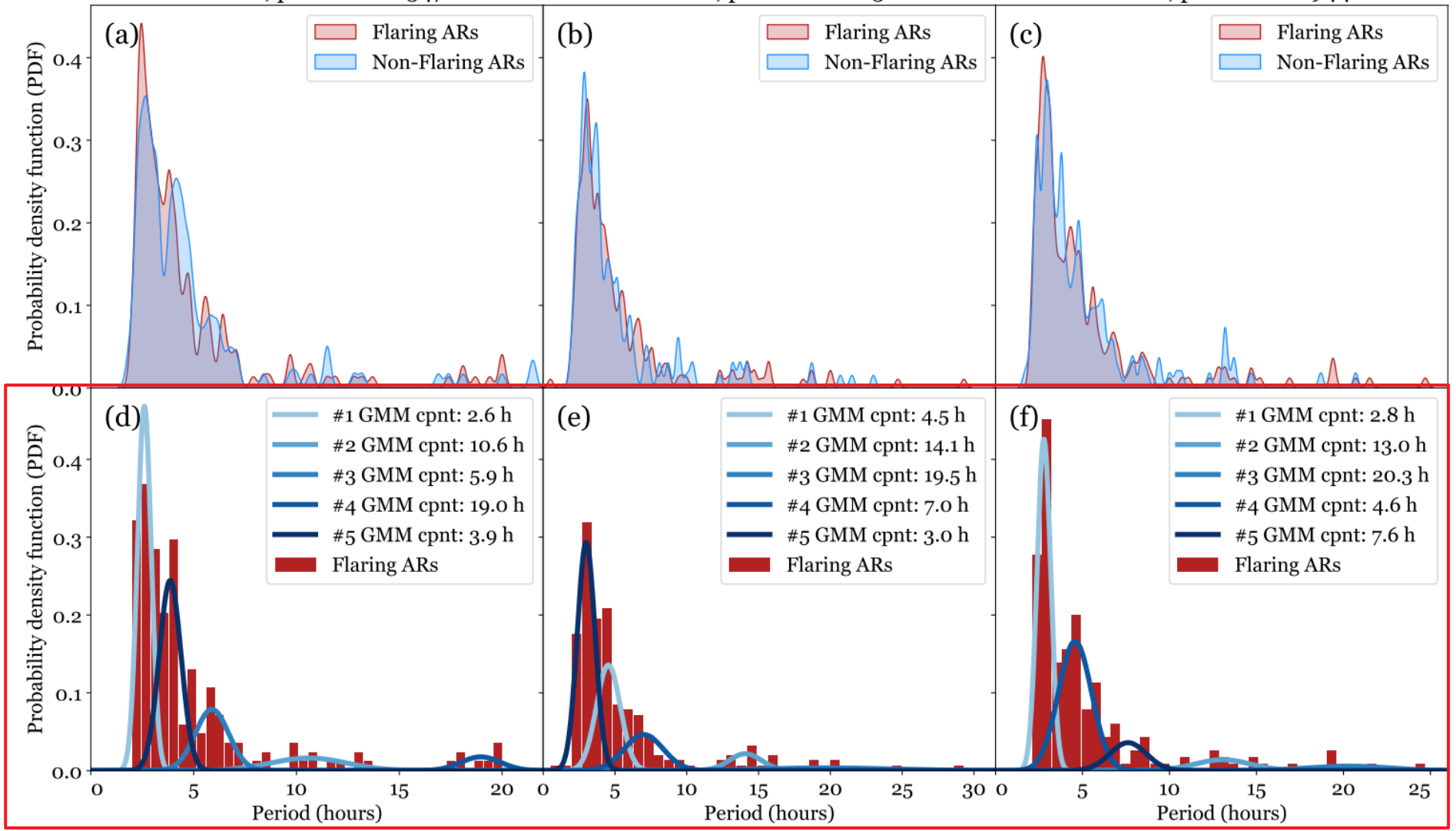
Emergence magnetic helicity flux
KS test, p-value = 0.547
Shearing magnetic helicity flux
KS test, p-value = 0.852
Total magnetic helicity flux
KS test, p-value = 0.944
(a)
(b)
(c)
Flaring ARs
Non-Flaring ARs
Probability density function (PDF)
(d)
(e)
(f)
#1 GMM cpnt: 2.6 h
#2 GMM cpnt: 10.6 h
#3 GMM cpnt: 5.9 h
#4 GMM cpnt: 19.0 h
#5 GMM cpnt: 3.9 h
#1 GMM cpnt: 4.5 h
#2 GMM cpnt: 14.1 h
#3 GMM cpnt: 19.5 h
#4 GMM cpnt: 7.0 h
#5 GMM cpnt: 3.0 h
#1 GMM cpnt: 2.8 h
#2 GMM cpnt: 13.0 h
#3 GMM cpnt: 20.3 h
#4 GMM cpnt: 4.6 h
#5 GMM cpnt: 7.6 h
Period (hours)

- **Errors** of the mean periods are estimated with bootstrap, re-sampled 10.000 times each.

Dashed black line shows the one-to-one correspondence between flaring and non-flaring periodicities.

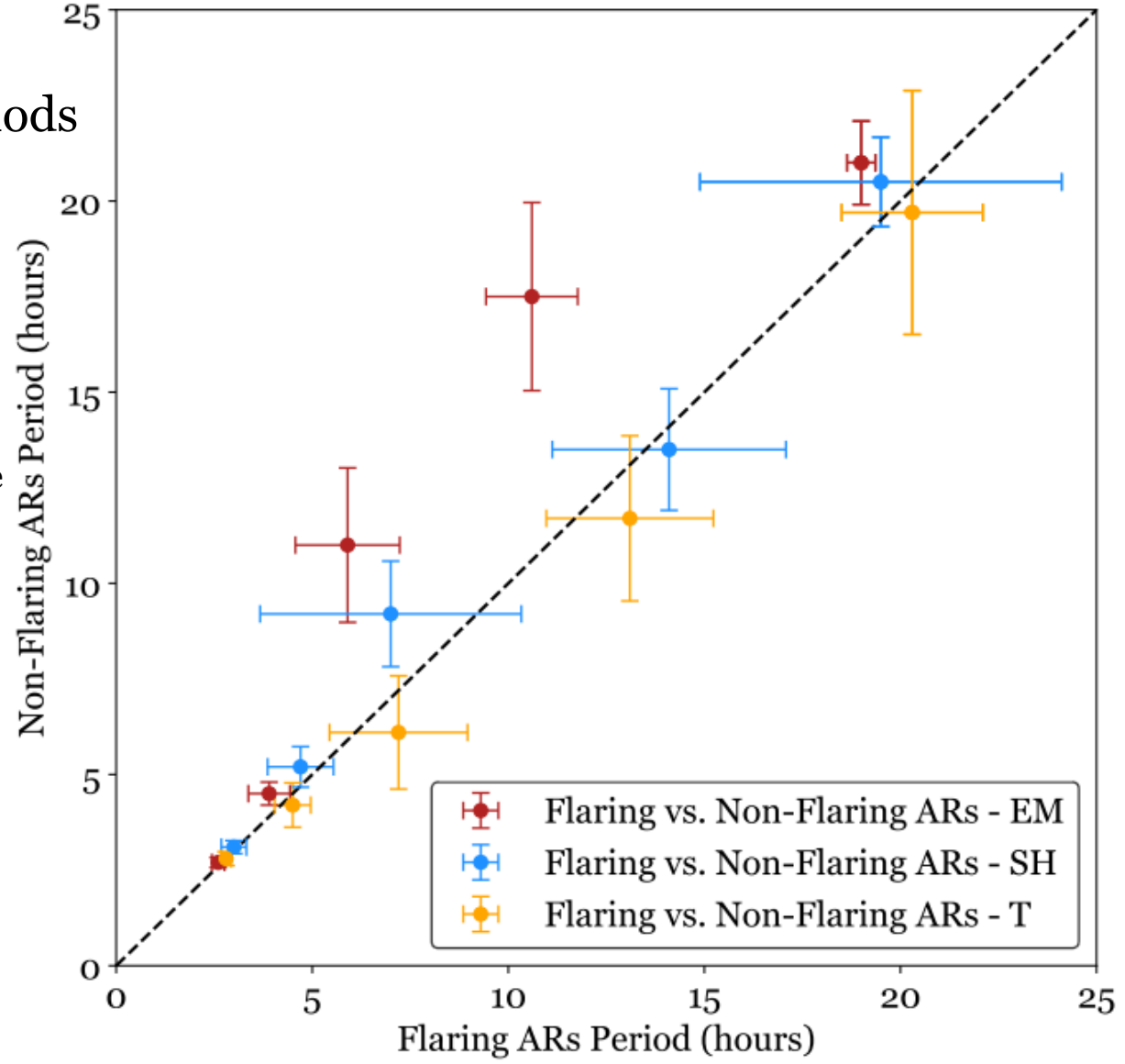

- **Errors** of the mean periods are estimated with bootstrap, re-sampled 10.000 times each.

Dashed black line shows the one-to-one correspondence between flaring and non-flaring periodicities.

- **EM periodicities are significantly deviated.**

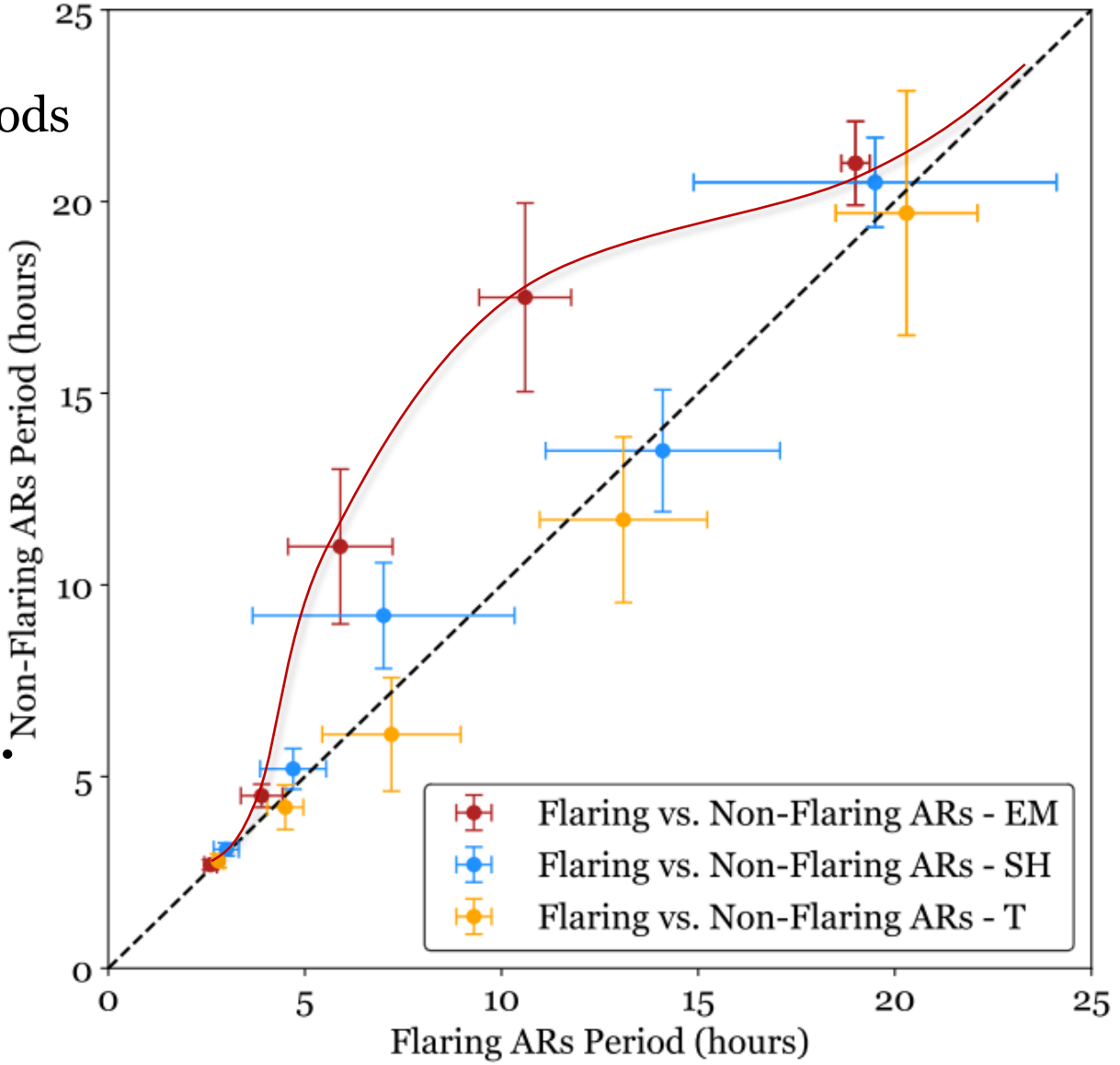

- **Errors** of the mean periods are estimated with bootstrap, re-sampled 10.000 times each.

Dashed black line shows the one-to-one correspondence between flaring and non-flaring periodicities.

- **EM periodicities are significantly deviated.**

- **EM** has a more **prominent role** in the flare-CME triggering processes.

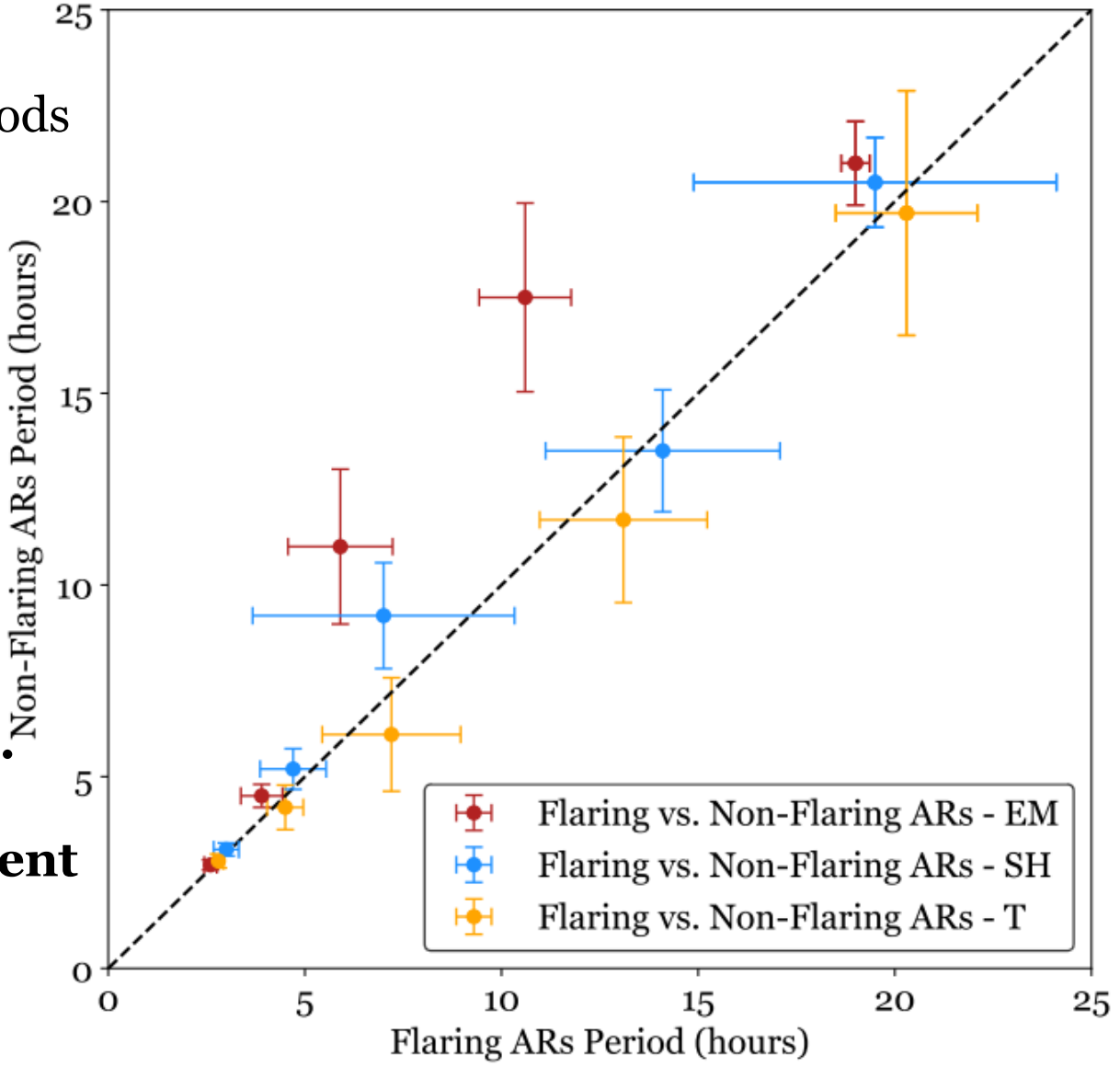

EM component

- We also **determined the harmonics** for each case of the period peaks of the oscillatory behaviour of EM/SH/T components.

EM component

- We also **determined the harmonics** for each case of the period peaks of the oscillatory behaviour of EM/SH/T components.

- From this, we can see that only the **peaks appearing in the EM of flaring ARs** are the ones that follow the properties of the harmonics well for an oscillatory **waveguide system**.

EM component

- We also **determined the harmonics** for each case of the period peaks of the oscillatory behaviour of EM/SH/T components.

- From this, we can see that only the **peaks appearing in the EM of flaring ARs** are the ones that follow the properties of the harmonics well for an oscillatory **waveguide system**.

- Such a **clear harmonic property** is not detected in the different flux components of flaring or non-flaring ARs.

Summary and Conclusions

- Analyzed the EM/SH/T evolution of **14 flaring and 14 non-flaring ARs**.

Summary and Conclusions

- Analyzed the EM/SH/T evolution of **14 flaring and 14 non-flaring ARs**.
- For flaring and non-flaring ARs, the EM/SH/T **periodicities occur in bands**.

(i) 2-9 hours, (ii) 11-14 hours, and (iii) 19-21 hours.

Summary and Conclusions

- Analyzed the EM/SH/T evolution of **14 flaring and 14 non-flaring ARs**.
- For flaring and non-flaring ARs, the EM/SH/T **periodicities occur in bands**.

(i) 2-9 hours, (ii) 11-14 hours, and (iii) 19-21 hours.

- The distribution of EM/SH/T peak periodicities were fitted using GMM.

Summary and Conclusions

- Analyzed the EM/SH/T evolution of **14 flaring and 14 non-flaring ARs**.
- For flaring and non-flaring ARs, the EM/SH/T **periodicities occur in bands**.

(i) 2-9 hours, (ii) 11-14 hours, and (iii) 19-21 hours.

- The distribution of EM/SH/T peak periodicities were fitted using GMM.
- The GMM-fitted EM peaks for flaring ARs shows **1/n-dependence** (n=1,2,3,...).

Summary and Conclusions

- Analyzed the EM/SH/T evolution of **14 flaring and 14 non-flaring ARs**.
- For flaring and non-flaring ARs, the EM/SH/T **periodicities occur in bands**.

  (i) 2-9 hours, (ii) 11-14 hours, and (iii) 19-21 hours.
- The distribution of EM/SH/T peak periodicities were fitted using GMM.
- The GMM-fitted EM peaks for flaring ARs shows **1/n-dependence** (n=1,2,3,...).
- The correlation between the central periodicities of the flaring and non-flaring ARs shows: **EM behaves significantly differently for flaring regions**.

Summary and Conclusions

- Analyzed the EM/SH/T evolution of **14 flaring and 14 non-flaring ARs**.
- For flaring and non-flaring ARs, the EM/SH/T **periodicities occur in bands**.

  (i) 2-9 hours, (ii) 11-14 hours, and (iii) 19-21 hours.
- The distribution of EM/SH/T peak periodicities were fitted using GMM.
- The GMM-fitted EM peaks for flaring ARs shows **1/n-dependence** (n=1,2,3,…).
- The correlation between the central periodicities of the flaring and non-flaring ARs shows: **EM behaves significantly differently for flaring regions**.
- The **presence of long periods** in EM and T suggests that the **EM component may play a crucial role in the formation of flares**, especially when:

Summary and Conclusions

- Analyzed the EM/SH/T evolution of **14 flaring and 14 non-flaring ARs**.
- For flaring and non-flaring ARs, the EM/SH/T **periodicities occur in bands**.

  (i) 2-9 hours, (ii) 11-14 hours, and (iii) 19-21 hours.
- The distribution of EM/SH/T peak periodicities were fitted using GMM.
- The GMM-fitted EM peaks for flaring ARs shows **1/n-dependence** (n=1,2,3,...).
- The correlation between the central periodicities of the flaring and non-flaring ARs shows: **EM behaves significantly differently for flaring regions**.
- The **presence of long periods** in EM and T suggests that the **EM component may play a crucial role in the formation of flares**, especially when:
  - the **AR has a δ-spot**,

Summary and Conclusions

- Analyzed the EM/SH/T evolution of **14 flaring and 14 non-flaring ARs**.
- For flaring and non-flaring ARs, the EM/SH/T **periodicities occur in bands**.

  (i) 2-9 hours, (ii) 11-14 hours, and (iii) 19-21 hours.
- The distribution of EM/SH/T peak periodicities were fitted using GMM.
- The GMM-fitted EM peaks for flaring ARs shows **1/n-dependence** (n=1,2,3,...).
- The correlation between the central periodicities of the flaring and non-flaring ARs shows: **EM behaves significantly differently for flaring regions**.
- The **presence of long periods** in EM and T suggests that the **EM component may play a crucial role in the formation of flares**, especially when:
  - the **AR has a δ-spot**,
  - **shorter** oscillatory **periods** appear **in** the **EM flux data**, and

Summary and Conclusions

- Analyzed the EM/SH/T evolution of **14 flaring and 14 non-flaring ARs**.
- For flaring and non-flaring ARs, the EM/SH/T **periodicities occur in bands**.

  (i) 2-9 hours, (ii) 11-14 hours, and (iii) 19-21 hours.
- The distribution of EM/SH/T peak periodicities were fitted using GMM.
- The GMM-fitted EM peaks for flaring ARs shows **1/n-dependence** (n=1,2,3,...).
- The correlation between the central periodicities of the flaring and non-flaring ARs shows: **EM behaves significantly differently for flaring regions**.
- The **presence of long periods** in EM and T suggests that the **EM component may play a crucial role in the formation of flares**, especially when:
  - the **AR has a δ-spot**,
  - **shorter** oscillatory **periods** appear **in** the **EM flux data**, and
  - these periods show the **presence of a harmonic oscillatory resonator**.